



HAL
open science

Kalman smoother for detection of heat sources defects

Mohamed Salim Bidou, Sylvain Verron, L. Perez, Laurent Autrique

► **To cite this version:**

Mohamed Salim Bidou, Sylvain Verron, L. Perez, Laurent Autrique. Kalman smoother for detection of heat sources defects. 2022 International Conference on Control, Automation and Diagnosis (ICCAD), Jul 2022, Lisbon, France. pp.1-6, 10.1109/ICCAD55197.2022.9853959 . hal-03789459

HAL Id: hal-03789459

<https://univ-angers.hal.science/hal-03789459>

Submitted on 15 Mar 2023

HAL is a multi-disciplinary open access archive for the deposit and dissemination of scientific research documents, whether they are published or not. The documents may come from teaching and research institutions in France or abroad, or from public or private research centers.

L'archive ouverte pluridisciplinaire **HAL**, est destinée au dépôt et à la diffusion de documents scientifiques de niveau recherche, publiés ou non, émanant des établissements d'enseignement et de recherche français ou étrangers, des laboratoires publics ou privés.

Kalman smoother for detection of heat sources defects

Mohamed Salim BIDOU

LARIS, Polytech, University of Angers
Angers, France
mohamedsalim.bidou@univ-angers.fr

Sylvain VERRON

LARIS, Polytech, University of Angers
Angers, France
sylvain.verron@univ-angers.fr

Laetitia PEREZ

LARIS, Polytech, University of Angers
Angers, France
laetitia.perez@univ-angers.fr

Laurent AUTRIQUE

LARIS, Polytech, University of Angers
Angers, France
laurent.autrique@univ-angers.fr

Abstract—This work is devoted to an application of the Kalman smoother method for the detection of failure times for a system of linear parabolic partial differential equation. For complex processes whose evolution is described by partial differential equations, the detection of failures is often difficult. In thermal systems, for example, when one or more heating sources fail, the sensors placed at a distance perceive the effect with delay. The Kalman smoother is then applied when the classical Kalman filter is used for the estimation of intensity of our sources. From these estimation, it is then necessary to determine the moment of failure and the possible restart of the heating. In the following, the whole problematic and the method of resolution is presented.

Index Terms—Fault detection, Kalman smoother, heat source, linear parabolic partial differential equations.

I. INTRODUCTION

Fault detection has become an attractive research topic in the past couple of decades due to increased complexity of industrial systems and elevated concerns about the safety of these systems, some faults can be viewed as malfunctions of the plant, sensor or actuators, that can lead to catastrophic scenarios.

In the context of complex physical systems, many phenomena are described by knowledge models based on partial differential equations. In thermal sciences, for example, heat exchange is described by Fourier's law, which leads to a system of parabolic partial differential equations (PDEs). In numerous references, characteristics of inverses problems and their numerical resolution are investigated [1] [2] [3].

Several difficulties must be mentioned. Firstly, some non-linear PDEs are difficult to deal with but are still essential for realistic physical situations. Secondly, the ill-posed nature of inverse heat conduction problem makes them particularly sensitive to measurement errors. Finally, the failures discussed below are of the "all-or-nothing" type and such discontinuous switching associated with the heat transport phenomenon places the framework of the study close to that of hybrid systems with delay.

The Kalman filtering (KF) technique [4] is one of the most widely used sequential algorithms, whose performance has

been widely verified in the state estimation of the different problems. Currently, Kalman filter has been deeply investigated for its application in inverse heat transfer problems. In [5] a constructed Kalman smoothing technique to solve the inverse estimation of radiation-conduction problem. In [6], [7], the author develops a methodology to estimate transient heat flux and temperature in a heat conduction problem in different 1D and 2D geometry using EKF coupled to RTS (EKS).

The application proposed in this article is an aluminium plate on which we will find 2 heating sources and 3 temperature sensors, all at a fixed location. For this type of application, treated by Bayesian filters, we can cite Orlande's works [8], [9]. In this particular work [8], the authors develop a methodology based on a Kalman filter making it possible to estimate at each moment the intensity and the position of a heating flux on a plate, allowing to estimate the trajectory of a source.

This article is composed as follows. Section 2 presents a description of the plate application and the modelling of the associated heat equations by the finite difference method. The 3th section comes to present in a theoretical way the Kalman filter as well as the Kalman smoother, and their use in our application in order to estimate the intensity of our sources. The 4th section presents how we will estimate the intensity of the sources to estimate the instants of starting and resumption of the sources, accompanied by numerical simulation results for different combinations and different noises of temperature sensor. Finally, we will conclude on the perspectives offered by this work.

II. APPLICATION DESCRIPTION AND MODELIZATION

A. Description of the physical problem

The application offered here is an aluminum plate 1m wide, 1m long and 3mm thick. On this plate are arranged 2 heating sources, as well as 3 temperature sensors. The 2 sources and the 3 sensors have known positions on the plate. The heating sources will behave erratically. Namely, these will experience all-or-nothing failures. Thus, a source could break down (its heat flux will then be zero) and then restart, and this several

times in a row. The problem with this application will be to estimate the instant(s) at which one or more sources will fail, as well as the instant(s) at which one or more sources will restart.

So, mathematically, we define the geometric domain as $\Omega \subset \mathfrak{R}^2$ and each point in space has coordinates $(x, y) \in \Omega$. In what follows $\Omega = [-0.5, 0.5]^2$ is the plate of 1 m side, in this domain is assumed to be thin enough to neglected temperature gradients with respect to the thickness denoted by e in m. The boundary of Ω is noted Γ . The time variable is $t \in T = [0, t_f]$. The temperature at any point in space is noted $\theta(x, y, t)$. The time evolution of temperature in the Ω domain is described by the following set of equations see [10]:

$$\begin{cases} \forall (x, y, t) \in \Omega \times T \\ \rho C \frac{\partial \theta}{\partial t} - \lambda \Delta \theta = \frac{\Phi - 2h(\theta - \theta_0)}{e} \\ \forall (x, y) \in \Omega \quad \theta(x, y, 0) = \theta_0 \\ \forall (x, y, t) \in \Gamma \times T \quad -\lambda \frac{\partial \theta}{\partial n} = 0 \end{cases} \quad (1)$$

where ρC is the volumic heat (product of the specific heat in $\text{J.kg}^{-1}.\text{K}^{-1}$ and the density in kg.m^{-3}), λ is the thermal conductivity (in $\text{W.m}^{-1}.\text{K}^{-1}$), $\Phi(x, y, t)$ is the heating flux (in W.m^{-2}), h the convective exchange coefficient in $\text{W.m}^{-2}.\text{K}^{-1}$ and $\theta_0(x, y)$ the ambient temperature (in K). The conditions at the edges are of the homogeneous Neumann type and correspond to adiabatic exchanges (a realistic situation given the extremely thin thickness e of the plate considered). For this application, we will consider the following parameters:

- aluminium plate
- volumic heat : $\rho C = 2.421 \times 10^6 \text{ J.K}^{-1}.\text{m}^{-3}$
- thermal conductivity : $\lambda = 178 \text{ W.m}^{-1}.\text{K}^{-1}$
- thickness : $e = 2 \times 10^{-3} \text{ m}$
- convective transfer coefficient : $h = 10 \text{ W.m}^{-2}.\text{K}^{-1}$
- initial temperature : $\theta_0(x, y) = 293 \text{ K}$
- final time : $t_f = 3600 \text{ s}$

Positions of the sources and sensors will be as follow: (represented in figure 1):

- the first source, S_1 is located at point $(x = 0.3; y = 0.3)$
- the second source, S_2 is located at point $(x = -0.4; y = -0.1)$
- the first sensor, C_1 is located at point $(x = 0.2; y = 0)$
- the second sensor, C_2 is located at point $(x = -0.1; y = 0.2)$
- the third sensor, C_3 is located at point $(x = -0.1; y = -0.2)$
- the number of heating flux is equal to $n_{heat} = 2$ and the number of sensors is equal to $n_{sensors} = 3$

The heat flux $\Phi(x, y, t)$ is provided by several heating sources:

$$\Phi(x, y, t) = \sum_{n=1}^{n_{heat}} \Phi_n(x, y, t) \quad (2)$$

Each heating source is defined as follows:

$$\Phi_n(x, y, t) = f_n(x, y)g_n(t)\chi_n(t) \quad (3)$$

The function $f_n(x, y)$ is the spatial support of the source n , which follows a Gaussian distribution around the point (x_n, y_n) as:

$$f_n(x, y) = \exp\left(-\frac{(x - x_n)^2 + (y - y_n)^2}{(5 \times 10^{-2})^2}\right) \quad (4)$$

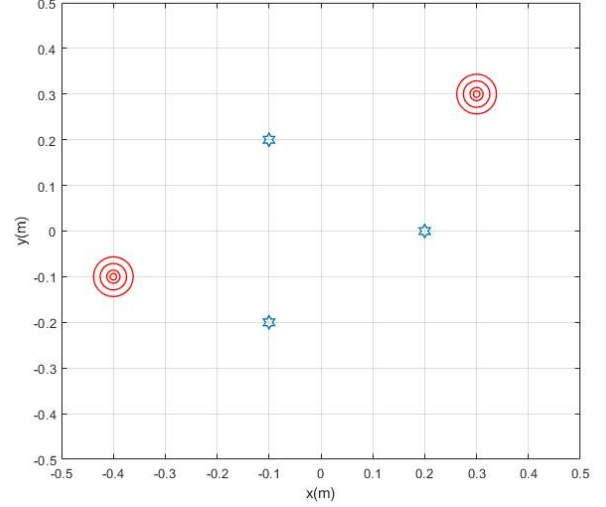


Fig. 1. Positions of the 2 sources and 3 sensors on the plate.

The function $g_n(t)$ describes the heating flux provided normally (without failure) by the source n . The heat flux for sources 1 and 2 are plotted on figure 2.

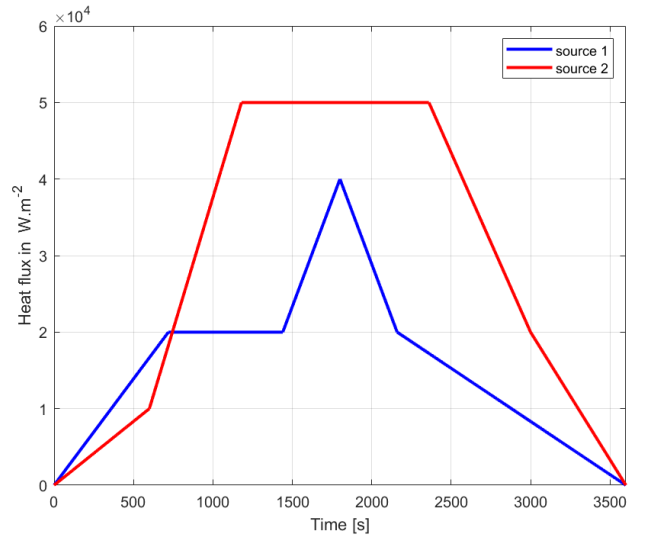


Fig. 2. Flux $g_1(t)$ and $g_2(t)$ of the two sources

The function $\chi_n(t)$ describes the possible failures of the heating source n :

$$\chi_n(t) = \begin{cases} 1 & \text{without fail} \\ 0 & \text{in case of default} \end{cases} \quad (5)$$

B. Approach of the problem by the finite difference method

The finite difference method see [11], [12] is one of the many techniques to obtain numerical solutions of equation 1. In all numerical solutions, the differential equation is replaced by a discrete approximation [12].

We define the temperature $\theta = \theta_{i,j}^k$ at point $\{x = i, y = j\}$ at time $t = k$, similarly for the heat flux in the same way, $\Phi = \Phi_{i,j}^k$.

$$\left[\frac{\partial \theta}{\partial t} \right]_{i,j}^k \simeq \frac{\theta_{i,j}^{k+1} - \theta_{i,j}^k}{\Delta t}, \quad \left[\frac{\partial^2 \theta}{\partial x^2} \right]_{i,j}^k \simeq \frac{\theta_{i-1,j}^k - 2\theta_{i,j}^k + \theta_{i+1,j}^k}{\Delta x^2}$$

$$\left[\frac{\partial^2 \theta}{\partial y^2} \right]_{i,j}^k \simeq \frac{\theta_{i,j-1}^k - 2\theta_{i,j}^k + \theta_{i,j+1}^k}{\Delta y^2}$$

In order to be mathematically exact, we assume that the discretized temperature introduce a little approximation.

An explicit discretization of Equation (1) using finite differences results in:

$$\theta_{i,j}^{k+1} = \alpha_1 \cdot \theta_{i,j}^k + \alpha_2 \cdot \theta_{i-1,j}^k + \alpha_2 \cdot \theta_{i+1,j}^k + \alpha_3 \cdot \theta_{i,j-1}^k + \alpha_3 \cdot \theta_{i,j+1}^k + \alpha_4 \cdot \Phi_{i,j}^k + \alpha_5 \quad (6)$$

where the subscripts (i, j) denote the finite difference node at $x_i = i\Delta x$, $i = 1, \dots, I$ and $y_j = j\Delta y$, $j = 1, \dots, J$ and the superscript k denotes the time $t_k = k\Delta t$, $k = 1, \dots, K$, where Δx , Δy and Δt are respectively the space and time steps. $\alpha_{l=1, \dots, 5}$, are constants (depending of the parameters of the application and discretization: $\Delta t, \Delta x, \Delta y, h, e, \rho, C, \lambda, \theta_0$).

The stability of the scheme (6) is due to Courant, Friedrichs, and Lewy condition (see [13]). This condition is necessary for the numerical scheme to produce a consistent solution when solving (6) numerically.

For computation facilities, we rewrite our problem in the form of a state evolution model by reordering sequentially all the nodes (i, j) with the index $m = 1, \dots, M$, where $M = I \times J$, giving:

$$\theta^{k+1} = A \cdot \theta^k + B \cdot G^k + H \quad (7)$$

Matrix A will be a square matrix coding the linear combination of θ terms with the different corresponding α_l coefficient.

The heat flux are assumed to be known at each time k :

$$G^k = \begin{bmatrix} g_1^k \\ g_2^k \end{bmatrix}$$

and their positions as well, allowing to have a flux vector on the whole domain: Φ^k

$$\alpha_4 \cdot \Phi^k = B \cdot G^k$$

The matrix $B [I \times J, n_{\text{heat}}]$ contains the spatial support of the source f_n , coding the positions of the gaussian distribution around the point (x_n, y_n) .

At a given frequency, we measure the temperature at certain points, these real measurements (thus subjected to an uncertainty / error of measurement) will be named θ_{obs}^k :

$$\theta_{obs}^k = \begin{bmatrix} \theta_{C_1}^k \\ \theta_{C_2}^k \\ \theta_{C_3}^k \end{bmatrix}$$

with $\theta_{C_h}^k$, $h = 1, 2, 3$ the scalar value given by the sensor C_h at time k . Logically, these observations reflect the real temperatures of the plate, so we can write:

$$\theta_{obs}^k = C \cdot \theta^k$$

The matrix C is a matrix composed of 0, except in h (3 in our case) element coding the positions of the sensors (the column gives the position of the sensor). For example:

$$C = \begin{bmatrix} 0 & 1 & \dots & 0 & 0 & 0 & \dots & 0 & 0 & 0 \\ 0 & 0 & \dots & 0 & 0 & 1 & \dots & 0 & 0 & 0 \\ 0 & 0 & \dots & 0 & 0 & 0 & \dots & 0 & 1 & 0 \end{bmatrix}$$

H a vector of length M with all elements equal to α_5 .

Our application is modeled as a state representation of a discrete time invariant linear system:

$$\begin{cases} \theta^{k+1} = A \cdot \theta^k + B \cdot G^k + H \\ \theta_{obs}^k = C \cdot \theta^k \end{cases} \quad (8)$$

It is assumed that a failure of source 1 occurred at $t = 1500s$. The evolution of the temperatures at the three sensors C_1, C_2, C_3 are shown in figure 3, assuming that the observations are subject to a Gaussian noise of mean zero and standard deviation $\sigma = 1^\circ C$.

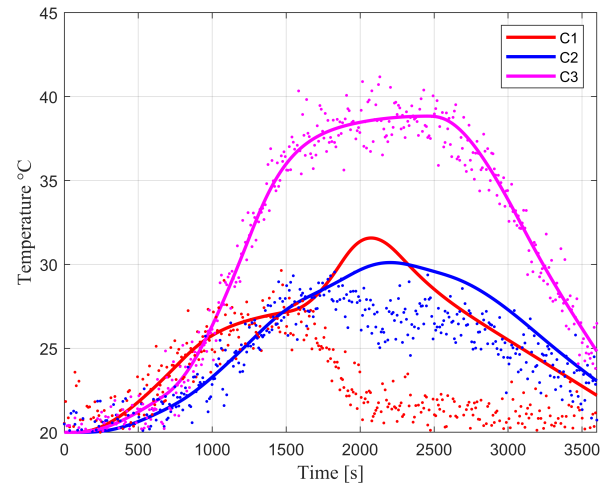


Fig. 3. Temperatures: without failure and without noise (continuous) and with failure and noise (points)

III. KALMAN FILTER AND SMOOTHER

The Kalman filter (see [4], [14], [15]) is used in a wide range of technological fields, very used in applications of control theory (speed/position estimation in particular), based on a system modeled as a state representation (continuous or discrete time).

For the application of the Kalman filter, we assumed that the evolution and observation models of a state vector \mathbf{X} (containing the variables to be dynamically estimated) are linear. Also, we assume that the noises in such models are Gaussian, with known means and covariances, and they are additive. Also, the evolution and observation models can be written, respectively, as follows:

$$\mathbf{X}_{k+1} = \mathbf{F}_{k+1}\mathbf{X}_k + \mathbf{S}_{k+1} + \mathbf{v}_k \quad (9)$$

$$\mathbf{Z}_k = \mathbf{H}_k\mathbf{X}_k + \mathbf{n}_k \quad (10)$$

where \mathbf{F} and \mathbf{H} are known matrices for the linear evolutions of state \mathbf{X} and observation \mathbf{Z} , respectively, and \mathbf{S} is a known vector for the state evolution model. Under the assumption that \mathbf{Q} and \mathbf{R} are gaussians, \mathbf{X} is also a gaussian with computable mean $\boldsymbol{\mu}$ and covariance $\boldsymbol{\Sigma}$. Assuming that the noises \mathbf{v} and \mathbf{n} have zero mean and covariance matrices \mathbf{Q} and \mathbf{R} , respectively, the prediction and update steps of the Kalman filter, for each $k = 1, \dots, \tau$, where $\tau = t_f / \Delta t_{obs}$ are given by:

Inputs: $\boldsymbol{\mu}_k, \boldsymbol{\Sigma}_k$ for each $k = 1, \dots, \tau$ computed by the Kalman filter algorithm.

- 1) Initialize: $\hat{\boldsymbol{\mu}}_{0|0}$ and $\boldsymbol{\Sigma}_{0|0}$.
- 2) For $k = 1, 2, \dots, \tau$:

Prediction :

$$\hat{\boldsymbol{\mu}}_{k|k-1} = \mathbf{F}_k \hat{\boldsymbol{\mu}}_{k-1|k-1} + \mathbf{S}_k \quad (11)$$

$$\hat{\boldsymbol{\Sigma}}_{k|k-1} = \mathbf{F}_k \hat{\boldsymbol{\Sigma}}_{k-1|k-1} \mathbf{F}_k^T + \mathbf{Q}_k \quad (12)$$

Update :

$$\mathbf{K}_k = \hat{\boldsymbol{\Sigma}}_{k|k-1} \mathbf{H}_k^T \left(\mathbf{H}_k \hat{\boldsymbol{\Sigma}}_{k|k-1} \mathbf{H}_k^T + \mathbf{R}_k \right)^{-1} \quad (13)$$

$$\hat{\boldsymbol{\mu}}_{k|k} = \hat{\boldsymbol{\mu}}_{k|k-1} + \mathbf{K}_k \left(\mathbf{Z}_k - \mathbf{H}_k \hat{\boldsymbol{\mu}}_{k|k-1} \right) \quad (14)$$

$$\hat{\boldsymbol{\Sigma}}_{k|k} = (\mathbf{I} - \mathbf{K}_k \mathbf{H}_k) \hat{\boldsymbol{\Sigma}}_{k|k-1} \quad (15)$$

where \mathbf{K}_k is the so-called Kalman's gain matrix, and \mathbf{Z}_k is the observation vector at instant k . We recall that in our application, temperatures are not observed at each instant (just every 9 seconds), and so in the case of no observation at instant k , then $\hat{\boldsymbol{\mu}}_{k|k} = \hat{\boldsymbol{\mu}}_{k|k-1}$.

In order to estimate the different instants of failure and recovery of the sources, we will assume that we study this application offline. In this case, a better estimation of the state vector could be obtained by the Kalman smoother (see [16]) also known under the name Rauch-Tung-Striebel (RTS) smoother [17]. For this algorithm, we suppose that we have already applied the Kalman filter, the backward steps are described as follows:

Inputs: $\hat{\boldsymbol{\mu}}_{\tau|\tau}, \hat{\boldsymbol{\Sigma}}_{\tau|\tau}$

- 1) For $k = \tau - 1, \tau - 2, \dots, 1$:

$$\begin{aligned} \mathcal{P}_k &= \hat{\boldsymbol{\Sigma}}_{k|k} \mathbf{F}_k^T \hat{\boldsymbol{\Sigma}}_{k+1|k}^{-1} \\ \hat{\boldsymbol{\mu}}_{k|\tau} &= \hat{\boldsymbol{\mu}}_{k|k} + \mathcal{P}_k (\boldsymbol{\mu}_{k+1|\tau} - \hat{\boldsymbol{\mu}}_{k+1|k}) \\ \hat{\boldsymbol{\Sigma}}_{k|\tau} &= \hat{\boldsymbol{\Sigma}}_{k|k} + \mathcal{P}_k (\boldsymbol{\Sigma}_{k+1|\tau} - \hat{\boldsymbol{\Sigma}}_{k+1|k}) \mathbf{C}_k^T \end{aligned}$$

For our problem, with the fact that our \mathbf{A} , \mathbf{B} and \mathbf{C} matrices are constant over the time, we can rewrite our equation (8) as follows :

$$\begin{cases} \boldsymbol{\theta}^{k+1} = \mathbf{A} \cdot \boldsymbol{\theta}^k + \mathbf{B} \cdot \mathbf{G}^k + \mathbf{H} + \mathbf{w}_k \\ \boldsymbol{\theta}_{obs}^k = \mathbf{C} \cdot \boldsymbol{\theta}^k + \mathbf{v}_k \end{cases} \quad (16)$$

In what follows, we want to estimate, not only $\boldsymbol{\theta}^k$, but especially the input \mathbf{G}^k (we can easily arrange the constant), \mathbf{v}_k and \mathbf{w}_k will allow to take into account respectively the sensor noises and the model noises.

In order to estimate the input vector \mathbf{G}^k , one approach is to redesign the Kalman filter so that the input vector is included in the state vector ([8], [18]):

$$\begin{cases} \boldsymbol{\theta}^{k+1} = \mathbf{A} \cdot \boldsymbol{\theta}^k + \mathbf{B} \cdot \mathbf{G}^k + \mathbf{H} + \mathbf{w}_k \\ \boldsymbol{\theta}_{obs}^k = \mathbf{C} \cdot \boldsymbol{\theta}^k + \mathbf{v}_k \end{cases} \quad (17)$$

⇓

$$\begin{cases} \begin{bmatrix} \boldsymbol{\theta}^{k+1} \\ \mathbf{G}^{k+1} \end{bmatrix} = \mathbf{A}' \cdot \begin{bmatrix} \boldsymbol{\theta}^k \\ \mathbf{G}^k \end{bmatrix} + \mathbf{H}' + \mathbf{w}'_k \\ \boldsymbol{\theta}_{obs}^k = \mathbf{C}' \cdot \begin{bmatrix} \boldsymbol{\theta}^k \\ \mathbf{G}^k \end{bmatrix} + \mathbf{v}_k \end{cases} \quad (18)$$

with

$$\mathbf{A}' = \begin{bmatrix} \mathbf{A} & \mathbf{B} \\ \mathbf{0} & \mathbf{I} \end{bmatrix} \quad \text{and} \quad \mathbf{C}' = [\mathbf{C} \quad \mathbf{0}] \quad (19)$$

For \mathbf{v}_k , it can be defined as a multivariate Gaussian variable (of dimension 3), with zero mean and variance-covariance matrix depending on the sensors

$$\boldsymbol{\mu}_v = \begin{bmatrix} 0 \\ 0 \\ 0 \end{bmatrix} \quad \boldsymbol{\Sigma}_v = \begin{bmatrix} \sigma_{C_1}^2 & 0 & 0 \\ 0 & \sigma_{C_2}^2 & 0 \\ 0 & 0 & \sigma_{C_3}^2 \end{bmatrix}$$

For \mathbf{w}_k , we can define it as a multivariate Gaussian variable (of dimension $\boldsymbol{\theta}$ by adding the dimension \mathbf{G}), with mean zero and the following variance matrix:

$$\boldsymbol{\mu}_w = \begin{bmatrix} 0 \\ 0 \\ \vdots \\ 0 \\ 0 \end{bmatrix}$$

$$\Sigma_w = \begin{bmatrix} \sigma_{\theta_{1,1}}^2 & 0 & 0 & 0 & 0 & 0 & 0 \\ 0 & \ddots & 0 & 0 & 0 & 0 & 0 \\ 0 & 0 & \sigma_{\theta_{i,j}}^2 & 0 & 0 & 0 & 0 \\ 0 & 0 & 0 & \ddots & 0 & 0 & 0 \\ 0 & 0 & 0 & 0 & \sigma_{\theta_{I,J}}^2 & 0 & 0 \\ 0 & 0 & 0 & 0 & 0 & \sigma_{g1}^2 & 0 \\ 0 & 0 & 0 & 0 & 0 & 0 & \sigma_{g2}^2 \end{bmatrix} \quad (20)$$

The application of this Kalman smoother algorithm, allows us to obtain \hat{g}_1^k and \hat{g}_2^k , respectively the estimate of g_1 and g_2 for each instant k . Now that we have \hat{g}_1^k and \hat{g}_2^k , we finally have to estimate the instants of failure and restart of each source: χ_1^k and χ_2^k (see equation (5)).

IV. FAILURE INSTANT ESTIMATION AND NUMERICAL SIMULATIONS

A. Failure and restart instants estimation

In order to estimate the failure instant t_{fail} , as well as the restart instant (t_{rest} , we will foremost estimate the vectors χ_1^k and χ_2^k . We will assume that the source failures are independent events, and so we can treat each source separately. We exploit the fact that we know the theoretical signal of each $g_n(t)$ without failure (see Figure 2). By constructing all possible χ_n vectors (with a failure instant t_{fail} and a restart instant t_{rest}), we will be able to compare the square error of \hat{g}_n with all the $g_n(t) \times \chi_{\text{cand}}$. The one with the lowest error will be chosen, giving its instants of failure and restart.

Thus, for each source, we can use the following algorithm:

- 1) Construct all χ_{cand} vectors, the candidate vectors with $t_{\text{fail}} = 1, 2, \dots, \tau$ and $t_{\text{rest}} = 1, 2, \dots, \tau$
- 2) For each χ_{cand} , compute $g_n(t) \times \chi_{\text{cand}}$
- 3) For each χ_{cand} , compute Square Error (SE) between $g_n(t) \times \chi_{\text{cand}}$ and \hat{g}_n
- 4) Select the χ_{cand} minimizing SE

B. Example

We propose to illustrate the proposed methodology with the example of a failure on the first source at $t = 1000s$ and a restart at $t = 2500s$, for a monitoring of 1 hour (3600s). Parameters are the following $\Delta x = \Delta y = 0.05m$, $\Delta t = 1s$, $\Delta t_{\text{obs}} = 9s$. The sources follow the same as described in figure 2.

First of all, we can plot the measurements (see figure 4). Once we have the measurements, we can apply the Kalman filter then the Kalman smoother. We obtained, for $g_1(k)$, the signals of figure 5. With the g_1 estimated by Kalman smoother, we can apply the search strategy described in the previous subsection. Figure 6 shows the different g_1 : theoretical (failure free), real (the theoretical with failure), the smoother estimate, and the best computed candidate. It can be seen that in this example, estimated instants of failure and restart are the following: $t_{\text{fail}} = 996s$ and $t_{\text{rest}} = 2533s$.

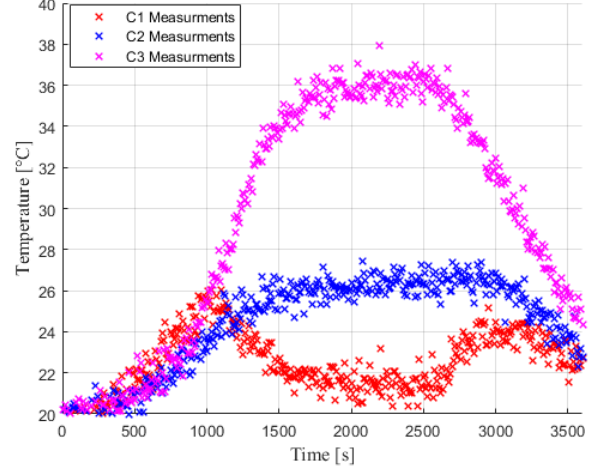


Fig. 4. Temperatures from sensors

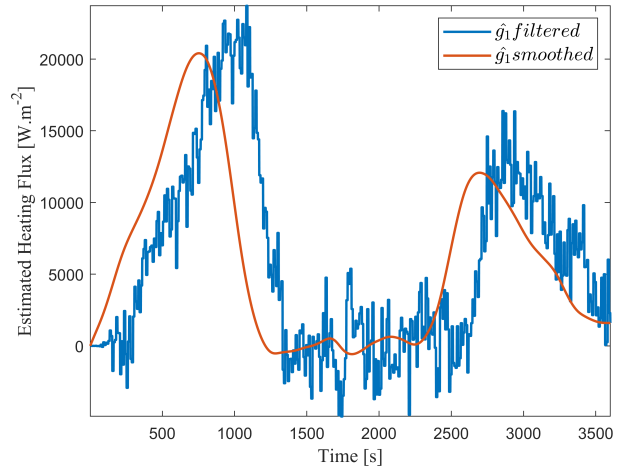


Fig. 5. g_1 estimated by Kalman filter and Kalman smoother

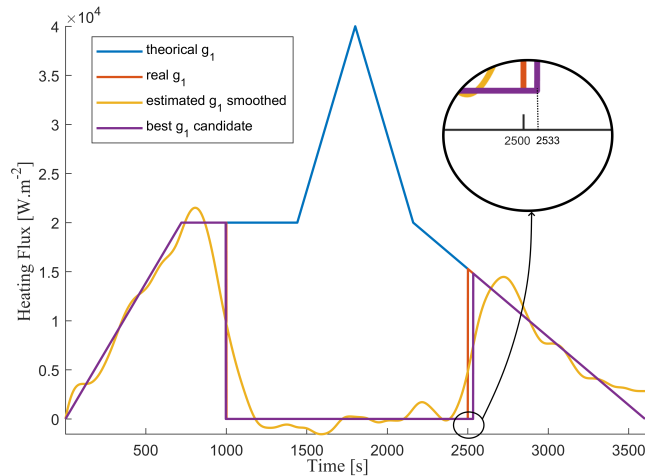


Fig. 6. Best g_1 candidate gives $t_{\text{fail}} = 996$ and $t_{\text{rest}} = 2533$

Now that the methodology has been described and that an example has been given, we could give some performances results in different configurations.

C. Results

In order to demonstrate the relevance of the proposed approach, different configurations has been simulated. Data have been taken from a Comsol simulation and analyzed with Matlab by our described methodology (preventing inverse crime). Discretization parameters are taken as $\Delta t = 1s$, $\Delta x = \Delta y = 0.05m$. As on a real system, the measurements at the three sensors are subject to an uncertainty described by a Gaussian noise of zero mean and different standard deviations σ are taken into account. So, results are given for 3 different level of noise: $\sigma = 0.1^\circ$, $\sigma = 0.5^\circ$ and $\sigma = 1^\circ$. So, in order to see the impact of such a parameter, for each configuration, we give results in term of mean and standard deviation (in brackets) on 30 simulations.

The first configuration is the simulation of a failure of the first source at $t = 1500s$. Results are given in the table I. We could clearly see that our approach gives good estimates of the failure instant, but, as expected, the greater the noise of the sensors, the worse the performance.

TABLE I
IDENTIFICATION OF FAILURE FOR DIFFERENT NOISE LEVELS

	Failure $t_{fail,1}^1$
$\sigma = 0.1^\circ C$	1500.03(1.426)
$\sigma = 0.5^\circ C$	1499.57(6.961)
$\sigma = 1^\circ C$	1501.30(13.63)

The second configuration is the simulation of a failure of the first source at $t = 1000s$ and a recovery at $t = 2500s$. Results are given in the table II.

TABLE II
IDENTIFICATION OF FAILURE AND RESTART TIMES FOR DIFFERENT NOISE LEVELS

	Failure $t_{fail,1}^1$	Restart $t_{rest,1}^1$
$\sigma = 0.1^\circ C$	1011.63(1.79)	2514.60(2.27)
$\sigma = 0.5^\circ C$	1013.43(8.29)	2513.27(10.87)
$\sigma = 1^\circ C$	1009.67(16.49)	2518.03(19.74)

In the last configuration, the goal is to demonstrate that source separation is possible. So, failures on the 2 sources are simulated at 2 different instants: we consider a failure of the first source at $t = 1000s$ and a failure instant of the second source at $t = 2000s$. Results are given in the table III.

TABLE III
IDENTIFICATION OF FAILURE TIMES FOR THE TWO SOURCES FOR DIFFERENT NOISE LEVELS

	Failure $t_{fail,1}^1$	Failure $t_{fail,2}^1$
$\sigma = 0.1^\circ C$	1011.87(1.61)	2010.03(0.81)
$\sigma = 0.5^\circ C$	1009.67(8.78)	2009.63(3.69)
$\sigma = 1^\circ C$	1021.60(18.51)	2013.67(4.69)

V. CONCLUSION

In this article, we have proposed a methodology allowing to estimate failure and restart of heat sources. This is done by the application of a Kalman smoother and a search strategy into different candidate signals of the source. Considering the fact that we monitor temperature with only 3 sensors distant of the sources, the approach gives very good results. Evidently, next work will be to take into account that heat sources could move on the plate.

REFERENCES

- [1] R. C. Aster, B. Borchers, and C. H. Thurber, *Parameter estimation and inverse problems*. Elsevier, 2018.
- [2] J. V. Beck and K. J. Arnold, *Parameter estimation in engineering and science*. James Beck, 1977.
- [3] A. Tarantola, *Inverse problem theory and methods for model parameter estimation*. SIAM, 2005.
- [4] R. E. Kalman, "A new approach to linear filtering and prediction problems," 1960.
- [5] S. Wen, H. Qi, Z.-T. Niu, L.-Y. Wei, and Y.-T. Ren, "Efficient and robust prediction of internal temperature distribution and boundary heat flux in participating media by using the kalman smoothing technique," *International Journal of Heat and Mass Transfer*, vol. 147, p. 118851, 2020.
- [6] N. Daouas and M.-S. Radhouani, "A new approach of the kalman filter using future temperature measurements for nonlinear inverse heat conduction problems," *Numerical Heat Transfer, Part B: Fundamentals*, vol. 45, no. 6, pp. 565–585, 2004.
- [7] N. Gaaloul and N. Daouas, "An extended approach of a kalman smoothing technique applied to a transient nonlinear two-dimensional inverse heat conduction problem," *International Journal of Thermal Sciences*, vol. 134, pp. 224–241, 2018.
- [8] H. Massard, H. Orlande, and O. Fudym, "Estimation of position-dependent transient heat source with the kalman filter," *Inverse Problems in Science and Engineering*, vol. 20, no. 7, pp. 1079–1099, 2012.
- [9] H. R. Orlande, M. J. Colaco, G. S. Dulikravich, F. Vianna, W. Da Silva, H. Fonseca, and O. Fudym, "State estimation problems in heat transfer," *International Journal for Uncertainty Quantification*, vol. 2, no. 3, 2012.
- [10] A. Vergnaud, L. Perez, and L. Autrique, "Quasi-online parametric identification of moving heating devices in a 2d geometry," *International Journal of Thermal Sciences*, vol. 102, pp. 47–61, 2016.
- [11] J. C. Strikwerda, *Finite difference schemes and partial differential equations*. SIAM, 2004.
- [12] M. N. Özisik, H. R. Orlande, M. J. Colaco, and R. M. Cotta, *Finite difference methods in heat transfer*. CRC press, 2017.
- [13] R. Courant, K. Friedrichs, and H. Lewy, "On the partial difference equations of mathematical physics," *IBM journal of Research and Development*, vol. 11, no. 2, pp. 215–234, 1967.
- [14] J. Kaipio and E. Somersalo, *Statistical and computational inverse problems*. Springer Science & Business Media, 2006, vol. 160.
- [15] M. N. Özisik and H. R. Orlande, *Inverse heat transfer: fundamentals and applications*. CRC press, 2021.
- [16] K. P. Murphy, *Machine learning: a probabilistic perspective*. MIT press, 2012.
- [17] H. E. Rauch, F. Tung, and C. T. Striebel, "Maximum likelihood estimates of linear dynamic systems," *AIAA journal*, vol. 3, no. 8, pp. 1445–1450, 1965.
- [18] D. Simon, *Optimal state estimation: Kalman, H infinity, and nonlinear approaches*. John Wiley & Sons, 2006.